PHYSICAL REVIEW C VOLUME 16, NUMBER 6 DECEMBER 1977

# Test of time reversal invariance in $^{57}$Fe†

N. K. Cheung,* H. E. Henrikson, and F. Boehm
*California Institute of Technology, Pasadena, California 91125*
(Received 5 August 1977)

An experiment has been performed to test time reversal invariance by observing the angular distribution of the linear polarization of the mixed $E2$ and $M1$ 122 keV $\gamma$ rays in $^{57}$Fe emitted from oriented $^{57}$Co nuclei. Nuclear orientation was achieved with a high magnetic field (the 288 kG hyperfine field of $^{57}$Co in an iron lattice) and a low temperature (16.5 to 18 mK obtained with a $^{3}$He-$^{4}$He dilution refrigerator). If time reversal invariance is violated, a term in the angular distribution of the form $(\vec{J}\cdot\vec{k}\times\vec{E})(\vec{J}\cdot\vec{k})(\vec{J}\cdot\vec{E})\sin\eta$ would be present, where the vectors $\vec{k}$ and $\vec{E}$ describe the propagation and linear polarization of the $\gamma$ ray, respectively, and $\vec{J}$ is the nuclear orientation vector. The quantity $\eta$ is the phase angle between the $E2$ and $M1$ matrix elements of the $\gamma$ transition. In our experiment the linear polarization was measured with a Compton polarimeter using an aluminum scatterer and NaI(Tl) detectors. From the observed asymmetry of $A=(-0.35\pm0.78)\times10^{-5}$, a value of $\sin\eta=(-3.1\pm6.5)\times10^{-4}$ was obtained. This result is consistent with time reversal invariance. Possible small contributions to the phase angle from atomic and nuclear final state effects are discussed.

[RADIOACTIVITY $^{57}$Fe; measured lin. pol. of 122 keV $\gamma$ from pol. nuclei. Deduced rel. phase of $E2$, $M1$.]

## I. INTRODUCTION

No breakdown of the time reversal symmetry in physics has ever been observed, aside from the famous case of the decay of the long-lived kaons. It has now been well established that in neutral kaon decay $CP$ invariance is not maintained.[1] $T$ violation is inferred via the $CPT$ theorem, whose validity is supported by experimental evidence. A further analysis of the kaon decay parameters suggests that $T$ is violated irrespective of $CPT$ symmetry.[2,3] It is thus of great interest to study the question of $T$ invariance with high accuracy in other systems, especially in the area of nuclear phenomena.

In low energy nuclear physics, time reversal noninvariant effects may manifest themselves in a mixed $\gamma$ transition. Let $A(L,\pi)$ and $A(L',\pi')$ be the reduced matrix elements of two interfering multipoles $(L,\pi)$ and $(L',\pi')$ in a $\gamma$ transition. The mixing ratio is defined as

$$\delta\equiv\frac{A(L,\pi)}{A(L',\pi')}\equiv|\delta|e^{i\eta}. \tag{1}$$

In the absence of final state interactions, $\eta$ would be different from 0 or $\pi$ if $T$ is violated.[4]

Previous experiments have established upper limits on $\sin\eta$ to a precision of a few parts in $10^3$. These results are close to the limits of $P$-even, $T$-odd observables predicted by the classes of $\Delta Y=0$ millistrong and electromagnetic theories[5,6] proposed to account for the observed $CP$ (and $T$) nonconservation. In the $K^0$ system it must be remembered that these theoretical limits are only crude estimates in the absence of a detailed theoretical formulation. With present experimental limits, the situation is unresolved and it is thus important to improve the experimental precision.

The sine of the phase angle $\eta$ appears in an observable which changes sign under the $T$ operation. The quantities we can measure are the nuclear spin $\vec{J}$, the photon momentum $\vec{k}$, the photon spin $\vec{S}$ (circular polarization), and the photon polarization vector $\vec{E}$. Any $T$-odd observable must involve a combination of at least three of these quantities. A table of $T$-odd observables can be found in Refs. 7 and 8. It turns out that most experiments involve a preparation of a polarized initial state (from which $\vec{J}$ is determined) and a measurement of two other quantities.

One type of experiment reported in the literature[9-11] is the $\beta$-$\gamma_1$-$\gamma_2$ triple correlations, where the polarization of the initial state $(\vec{J})$ is determined by measuring a preceding $\beta$ decay. In these experiments, $T$-odd quantities of the form $(\vec{k}_1\cdot\vec{k}_2\times\vec{k}_\beta)(\vec{k}_1\cdot\vec{k}_2)$ are sought. Because of the extremely low coincidence rates in a triple-correlation experiment, this method has been capable of achieving a precision of only about $10^{-2}$.

In another type of experiment,[12-17] the polarization of the initial state has been achieved by either capturing polarized thermal neutrons or by cooling the nuclei to low temperature under a strong magnetic field. The correlation of two cascade transitions (directions $\vec{k}_1$ and $\vec{k}_2$) from the polarized nuclei is then measured. Here terms of the form

$(\vec{J}\cdot\vec{k}_1\times\vec{k}_2)(\vec{k}_1\cdot\vec{k}_2)$ are searched, where $\vec{J}$ is the polarization of the initial state. Since $\vec{J}$ is known initially, only two quantities are actually measured. The low coincidence rate, though very much higher than that for a triple correlation, limits the precision to about a few parts in $10^3$.

If the linear polarization $\vec{E}$ is determined in addition to the $\gamma$-ray direction $\vec{k}$, $T$-odd terms of the form $(\vec{J}\cdot\vec{k}\times\vec{E})(\vec{J}\cdot\vec{k})(\vec{J}\cdot\vec{E})$ can be explored. This has been achieved by measuring the absorption of linearly polarized recoiless $\gamma$ rays in a magnetic medium.[18-20] Being essentially a single counting experiment, it is capable of achieving high precision [e.g., for the 90 keV transition in $^{99}$Ru, a result of $\sin\eta=(1.0\pm1.7)\times10^{-3}$ was reported]. Nevertheless, this method is limited to a few suitable Mössbauer cases and since they involve low energy ($\lesssim$100 keV) photons with large conversion amplitudes, final state interactions which simulate time-reversal effects are significant and the results are difficult to interpret.

We describe in this paper the results of an experiment aimed at the study of the term $(\vec{J}\cdot\vec{k}\times\vec{E})\times(\vec{J}\cdot\vec{k})(\vec{J}\cdot\vec{E})$ in the angular distribution of a $\gamma$ ray $\vec{k}$ emitted from nuclei polarized by low temperature nuclear orientation. With this method a considerably lower limit on $T$ nonconservation in nuclear physics was attained. An abbreviated account of the experiment has been given earlier.[21]

## II. PRINCIPLES OF THE EXPERIMENT

The angular and linear polarization distribution for a mixed electromagnetic transition from oriented nuclei with spin $J_0$ can be written as a sum of three terms[22,23];

$$W(\theta,\phi)=W_1(\theta)+W_2(\theta,\phi)+W_3(\theta,\phi), \tag{2}$$

where $\theta$ is the angle between the momentum vector $\vec{k}$ of the $\gamma$ ray and the orientation axis $\vec{J}$, and $\phi$ is the angle between the linear polarization vector $\vec{E}$ and the plane formed by $\vec{J}$ and $\vec{k}$.

$W_1(\theta)$ is the usual directional distribution term, if the linear polarization is not measured, and is given by

$$W_1(\theta)=\sum_{k=\text{even}} Q_k B_k(J_0) U_k A_k P_k(\cos\theta). \tag{3}$$

$B_k$ is the orientation tensor which depends on $J_0$ and the populations $P(m)$ of the $m$ levels of the nucleus. $U_k$ describes the deorientation of the decaying level due to previous transitions. $A_k$ is the angular distribution coefficient for the $\gamma$ transition and depends on the spins of the initial and final states ($J_i$ and $J_f$). $P_k(\cos\theta)$ is the Legendre polynomial of order $k$, and $Q_k$ is the solid angle correction. The coefficients $B_k$, $U_k$, and $A_k$ have been tabulated for example by Krane.[24,25]

$W_2(\theta,\phi)$ is the usual $T$-even linear polarization distribution term and $W_3(\theta,\phi)$ is the $T$-odd linear polarization term of particular interest to us. These two terms are given by

$$W_2(\theta,\phi)=\sum_{k=\text{even}} Q_k B_k U_k A_{k2}\, 2\left[\frac{(k-2)!}{(k+2)!}\right]^{1/2} \times P_k^{\,2}(\cos\theta)\cos2\phi, \tag{4}$$

$$W_3(\theta,\phi)=\sum_{k=\text{odd}} Q_k B_k U_k A'_{k2}(-2i)\left[\frac{(k-2)!}{(k+2)!}\right]^{1/2} \times P_k^{\,2}(\cos\theta)\sin2\phi, \tag{5}$$

with $A_{k2}$ and $A'_{k2}$ given by

$$A_{k2}=-\frac{E_p}{2}\,\frac{-f_k(LL)F_k(LLJ_fJ_i)-2f_k(LL')F_k(LL'J_fJ_i)|\delta|\cos\eta+|\delta|^2 f_k(L'L')F_k(L'L'J_fJ_i)}{1+|\delta|^2}, \tag{6}$$

$$A'_{k2}=-(E_p/2)f_k(LL')F_k(LL'J_fJ_i) \times[2i|\delta|\sin\eta/(1+|\delta|^2)], \tag{7}$$

where

$$f_k(LL')\equiv\begin{pmatrix} L & L' & k\\ -1 & -1 & 2\end{pmatrix}\Big/\begin{pmatrix} L & L' & k\\ 1 & -1 & 0\end{pmatrix}. \tag{8}$$

$F_k$'s are the usual $F$ coefficients in electromagnetic transitions, and $E_p$ is the polarization efficiency for detecting linear polarization.

The time reversal transformation

$$\vec{k}\to-\vec{k},\quad \vec{J}\to-\vec{J},\quad \text{and } \vec{E}\to\vec{E} \tag{9}$$

corresponds to a geometrical transformation of $\theta\to\pi-\theta$ and $\phi\to\phi+\pi$ in Eqs. (2)–(5), and it is evident that $W_1$ and $W_2$ are $T$-even while $W_3$ is $T$-odd. We also see from (5) and (7) that the lowest nonvanishing term in $W_3$ has $k=3$ and is proportional to $\sin^2\theta\cos\theta\sin2\phi$. This term is proportional to the $T$-odd quantity $(\vec{J}\cdot\vec{k}\times\vec{E})(\vec{J}\cdot\vec{k})\times(\vec{J}\cdot\vec{E})$ of interest to us. The magnitude of this term is a maximum for $\theta_{\max}=54.7^\circ$ or $\pi-54.7^\circ$ and $\phi=\pm45^\circ$.

The case we have chosen for the present experiment is the 122 keV $M1$-$E2$ transition in $^{57}$Fe emitted following the electron capture decay of $^{57}$Co. The decay scheme is shown in Fig. 1. $^{57}$Co has a large magnetic moment $\mu$ of $4.73\mu_N$ (Ref. 26) and a hyperfine field $H$ in iron of 288 kG (Ref.

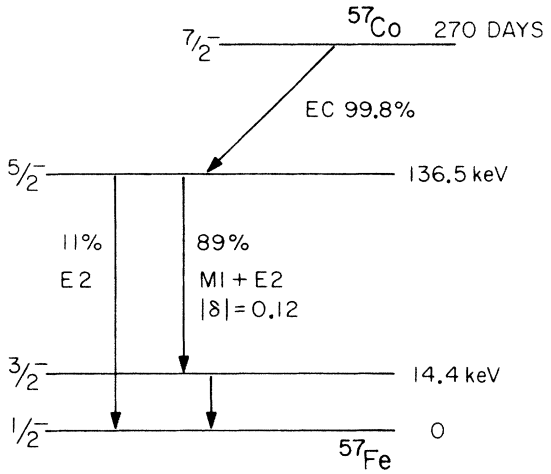


FIG. 1. Decay scheme of $^{57}$Co.

27), giving a value $\Delta = \mu H/J_0 k_B = 14.3$ mK; this is within the capability of our dilution refrigerator. The quantities $J_0$ and $k_B$ are the spin of the oriented state and the Boltzmann constant, respectively. The only somewhat unfavorable quantity in this case is the small mixing ratio, real $\delta = 0.120 \pm 0.001$ (Ref. 26). Nuclear orientation of $^{57}$Co in iron has been exhaustively studied in a previous work[26] as a preparation for the present experiment.

Applying the time reversal operation $\theta_{max} \rightarrow \pi - \theta_{max}$ and defining the asymmetry $A$ as shown, we find the following expression in our case:

$$A = \frac{W(\theta_{max}, \phi) - W(\pi - \theta_{max}, \phi)}{W(\theta_{max}, \phi) + W(\pi - \theta_{max}, \phi)}$$

$$= (-0.0164 E_p Q_3 B_3 P_3^2(\cos\theta_{max}) \sin 2\phi \sin\eta)/D, \quad (10)$$

where

$$D = 1 + 0.0058 Q_4 B_4 P_4(\cos\theta_{max}).$$

Since, as will be explained later, the pure $E2$ 136 keV line (11% intensity) cannot be resolved from the 122 keV line (89% intensity) in our experiment, $D$ was replaced by $D' = 1.124 - 0.039 Q_4 B_4 P_4(\cos\theta_{max})$.

Notice that the sign of $B_3$ is important in ascertaining the correct sign of $\sin\eta$. For $^{57}$Co, if we choose the positive direction of the externally applied magnetic field as the positive direction of the quantization axis, and $\theta$ is measured from this positive direction, $B_3$ is positive.[28]

A Compton polarimeter was used to measure the linear polarization of the $\gamma$ rays. Its sensitivity to the linear polarization is given by the Klein-Nishina formula for the differential cross section of Compton scattering:

$$\frac{d\sigma}{d\Omega} = \frac{1}{2} r_0^2 \left(\frac{E'}{E}\right)^2 \left(\frac{E'}{E} + \frac{E}{E'} - 2\sin^2\rho\cos^2\Psi\right). \quad (11)$$

The energy $E'$ of the scattered $\gamma$ ray is related to the energy $E$ of the incident $\gamma$ ray by

$$E' = E/[1 + (E/m_0c^2)(1 - \cos\rho)]. \quad (12)$$

$\rho$ is the scattering angle and $\Psi$ is the angle between the plane of polarization of the incident $\gamma$ ray and the scattering plane. $r_0$ is the classical radius of the electron and $m_0c^2$ is the electron rest energy of 511 keV. From Eq. (11), we see that a linearly polarized $\gamma$ ray is preferentially scattered perpendicular to its plane of polarization.

The polarization efficiency $E_p$ is defined by

$$E_p \equiv \frac{\frac{d\sigma}{d\Omega}(\rho = 90°, \Psi = 0°) - \frac{d\sigma}{d\Omega}(\rho = 90°, \Psi = 90°)}{\frac{d\sigma}{d\Omega}(\rho = 90°, \Psi = 0°) + \frac{d\sigma}{d\Omega}(\rho = 90°, \Psi = 90°)} \quad (13)$$

averaged over the solid angles.

For an infinitesimal solid angle and $E = 122$ keV, Eq. (13) gives $E_p = -0.96$. However, for a finite solid angle, $E_p$ will be very much reduced and has to be determined by measurements with a beam of known linear polarization or from Monte Carlo calculations.

## III. EXPERIMENTAL METHODS

### A. Source preparation and cryogenic apparatus

Carrier free $^{57}$Co with specific activity of 8.5 Ci/mg Co at 100% isotopic enrichment was obtained commercially from ICN.[29] It was supplied in the form of a 0.5 $N$ HCl solution. A tiny droplet of the solution was deposited on an iron disc of 3.2 mm diam and 12.7 $\mu$m thickness, dried under a heat lamp and diffused into iron at 890 °C in a hydrogen atmosphere. This process was repeated until a source strength of 2 mCi was attained. After a further diffusion of three to four days, the disc was etched with 1 $N$ HCl and washed with alcohol.

The annealed disk was soldered in a horizontal plane to the tip of a copper source rod using gallium solder [$H_c(T=0)$ is 50 G for Ga]. The upper end of the source rod was then screwed into the mixing chamber of the dilution refrigerator.[30] The source was located at the center of two pairs of superconducting magnet coils in a Helmholtz-type geometry (Fig. 2). The coils were not immersed in liquid helium but were thermally connected to the wall of the aluminum 4 K shield. The iron disk required a field of about 1.5 kG to sat-

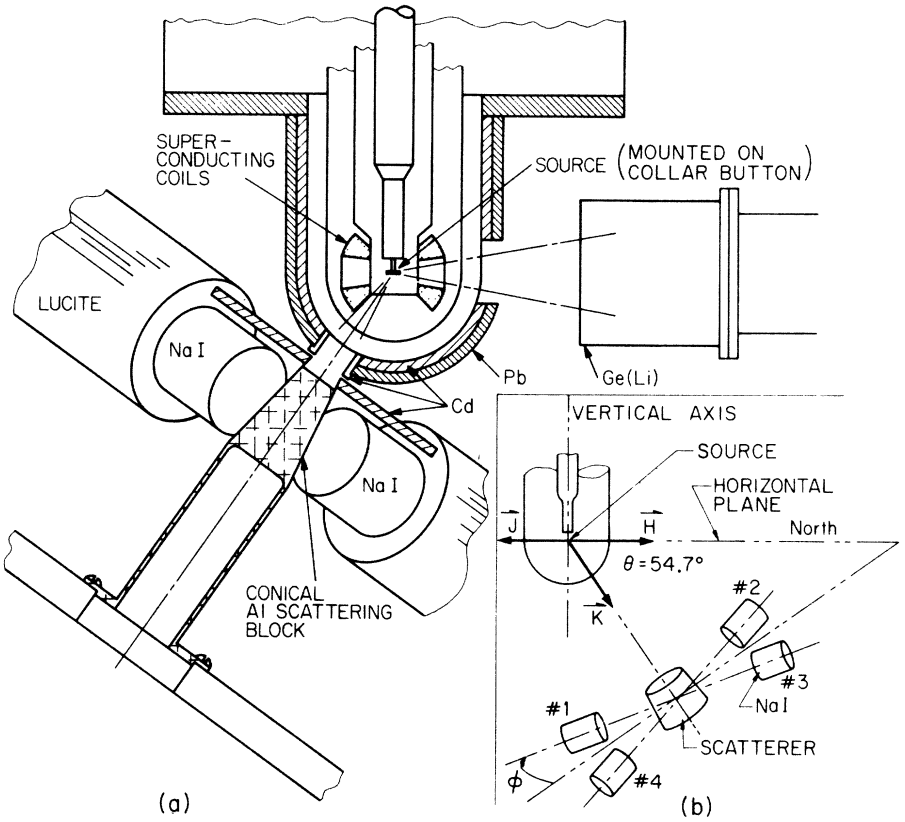


FIG. 2. Diagram showing the polarimeter and its geometry relative to the source and magnet positions. Only two of the four NaI detectors of the polarimeter are shown in the main diagram.

urate magnetically. Approximately 2 kG were used throughout the experiment.

### B. Compton polarimeter

The polarimeter consisted of an aluminum scatterer and four NaI(Tl) counters mounted at 90° to each other to detect the $\gamma$ rays that were scattered at $\rho = 90°$ from the incident beam. Details of the polarimeter and the physical setup are shown in Fig. 2. The NaI(Tl) detectors were shielded from the direct beam by a cadmium lined lead cup covering the tail piece of the refrigerator, leaving small exit windows for the $\gamma$ rays. The cadmium lining greatly attenuated the lead fluorescent x rays seen by the Na(I) detectors.

The magnetic effects on the photomultipliers were reduced to an insignificant amount by inserting a 30 cm Lucite light pipe between the NaI and the magnetically shielded photomultipliers. For a four-prong polarimeter symmetrically placed around the scatterer, any first order systematic errors such as those due to deviations from the precise scattering angles can be eliminated. A spectrum of the 90° scattered peak, relative to the unscattered 122 keV peak is shown in Fig. 3. The solid angle correction $Q_k$, for the polarimeter, was determined by conventional means to be $Q_2 = 0.982$, $Q_3 = 0.963$, and $Q_4 = 0.940$.

### C. Determination of the polarization efficiency $E_p$

#### *1. Monte Carlo calculation*

A Monte Carlo calculation was carried out to estimate the polarization and detection efficiencies and to compare the merits of different materials as scatterer, its size, etc. From Eq. (10) we see that for a given number of counts $N$, the sensitivity of the $T$-odd term is given by

$$\Delta(\sin\eta) \propto [-B_3(T) E_p \sqrt{\epsilon}\, \sqrt{N}]^{-1}, \tag{14}$$

where $\epsilon$ is the detection efficiency of the polarimeter. The quantity $-E_p\sqrt{\epsilon}$ therefore serves as a useful figure of merit for a given polarimeter (see also Ref. 31). In the Monte Carlo calculation, the distance between the scatterer and the detector $d$ could be varied at will to study how $E_p$ and $E_p\sqrt{\epsilon}$ vary with $d$. It turned out that $-E_p\sqrt{\epsilon}$ was a maximum when the detector was touching the scatter-

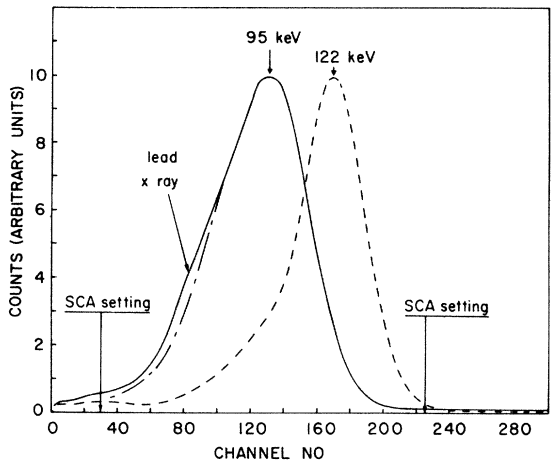


FIG. 3. Spectrum of the 90° Compton scattered peak. For comparison, the 122 keV photopeak spectrum is also included (dotted line). Also indicated is the single channel window.

er. The following results for $d=0$ cm were obtained:
aluminum scatterer

$$E_p = -0.400 \pm 0.010 - E_p\sqrt{\epsilon} = 0.150 \pm 0.005 ,$$

graphite scatterer

$$E_p = -0.380 \pm 0.010 - E_p\sqrt{\epsilon} = 0.135 \pm 0.004 .$$

(The "error" in these numbers is the standard deviation of $n$ runs divided by $\sqrt{n}$.)

*2. Measurements from oriented $^{57}$Co*

The most accurate determination of $E_p$ was obtained by utilizing the high degree of linear polarization in the $\gamma$ rays emitted from oriented $^{57}$Co. Since the weaker 136 keV line cannot be resolved from the 122 keV line in the scattered spectrum, we recorded the combined distribution of both lines. The pure $E2$ 136 keV transition has an opposite polarization pattern compared to the predominantly $M1$ 122 keV line and hence dilutes the net polarization of the latter. Taking the intensity ratio between the 122 and 136 keV lines to be 89 : 11 (Ref. 32) and assuming that the polarimeter has the same polarization efficiency for both lines, we obtain for the asymmetries as follows:

$$A(\theta=90^\circ) = \frac{W(\theta=90^\circ,\phi=0^\circ) - W(\theta=90^\circ,\phi=90^\circ)}{W(\theta=90^\circ,\phi=0^\circ) + W(\theta=90^\circ,\phi=90^\circ)}$$

$$= E_p \frac{0.492Q_2B_2 - 0.024Q_4B_4}{1.124 - 0.034Q_2B_2 - 0.014Q_4B_4} , \quad (15)$$

$$A(\theta=54.7^\circ) = \frac{W(\theta=54.7^\circ,\phi=0^\circ) - W(\theta=54.7^\circ,\phi=90^\circ)}{W(\theta=54.7^\circ,\phi=0^\circ) + W(\theta=54.7^\circ,\phi=90^\circ)}$$

$$= E_p \frac{0.328Q_2B_2 + 0.021Q_4B_4}{1.124 + 0.015Q_4B_4} . \quad (16)$$

Measurements were made with the polarimeter set at $\theta=54.7^\circ$ as well as $\theta=90^\circ$. The data were taken at $T=17.2$ mK where $B_2$ was 0.769 and $B_4$ was 0.110. The raw asymmetry for $\theta=90^\circ$ was $-0.145 \pm 0.001$, giving a raw $E_p$ of $-0.430 \pm 0.003$. The raw asymmetry for $\theta=54.7^\circ$ was $= -0.097 \pm 0.001$ giving a raw $E_p$ of $-0.434 \pm 0.005$, in excellent agreement with the $\theta=90^\circ$ data.

The presence of x rays dilutes the actual asymmetry of the effect to be measured in the following way. Let $N_1, N_2$ be the genuine counts of interest and $m_1, m_2$ the number of counts due to x rays. The measured asymmetry is then

$$A' = \frac{N_1+m_1-N_2-m_2}{N_1+m_1+N_2+m_2} \simeq \frac{N_1-N_2}{N_1+N_2}\frac{1}{1+f} = A\frac{1}{1+f} , \quad (17)$$

where $A$ is the true asymmetry, $A'$ is the measured asymmetry and $f \equiv (m_1+m_2)/(N_1+N_2)$. Assuming that the factors $f$ are the same in the polarization efficiency measurement as in the time reversal runs, we have two modifications to make:

$$A = A'(1+f) \quad \text{and} \quad E_p = E_p'(1+f) ; \quad (18)$$

$E_p$ is the true polarization efficiency and $E_p'$ the uncorrected polarization efficiency. Since $A$ is related to $\sin\eta$ by $A = CE_p \sin\eta$, $C$ being constant, we see that the final results for $\sin\eta$ and $\Delta(\sin\eta)$ are *not* affected by the x-ray correction. $f$ was determined by extrapolating the upper part of the low energy slope downward. All counts above the extrapolated curve were taken as x-ray events (Fig. 3). The result is $f=0.06 \pm 0.02$. Applying the x-ray correction factor we find $E_p = -0.456 \pm 0.009$.

D. Temperature measurement

In Eq. (10), [also Eqs. (15) and (16) as well], the orientation parameter $B_3$ and $B_4$ are functions of temperature. The source temperature had to be separately determined by measuring the directional distributions as given by Eq. (3). An Ortec planar Ge(Li) detector was placed at the side of the source opposite to the polarimeter to record the $\gamma$ ray pulse height spectrum. The nuclei were first oriented parallel to the axis of the detector (0°) and then perpendicular to it (90°). The areas under the photopeaks were calculated. From the ratio

$$B = \frac{2[N(0^\circ)-N(90^\circ)]}{N(0^\circ)+2N(90^\circ)} = \frac{B_2Q_2U_2A_2 + (5/12)B_4Q_4U_4A_4}{1+(7/12)B_4Q_4U_4A_4} \quad (19)$$

for the pure $E2$ 136 keV line, the temperature $T$ was determined by a numerical solution yielding a consistent set of values for $B_2(T)$ and $B_4(T)$.

Once $T$ was known, $B_3(T)$ could then be calculated. To check the consistency of the calculation and the measurement itself, the mixing ratio real $\delta$ of the 122 keV line was also evaluated and compared to the best experimental value of $0.120 \pm 0.001$.[26] $Q_2$ and $Q_4$ in Eq. (19) are the solid angle corrections for the finite size of the Ge(Li) detectors as determined from a previous work.[26]

The temperature was normally measured once every twenty-four hours. However, the 122 keV and 136 keV lines from the Ge(Li) detectors were monitored with a single channel analyzer throughout the time reversal run to check on the temperature stability and other changes that might occur. Except for the short period after filling liquid helium to the main reservoir and 1 K pot, the temperature fluctuation was found to be less than 0.2 mK during a 12 h run.

### E. Experimental setup and data acquisition for the time reversal runs

The physical setup of the experiment is shown in Fig. 2. The disk shaped source is seen as a line in the horizontal plane. The polarimeter is clamped on a pedestal allowing it to rotate by an angle $\phi$ about its axis of symmetry. For any one of the NaI counters the angle $\phi$ was fixed at 45° measured from the $\vec{j}, \vec{k}$ plane during all runs. The angle $\theta$ between the horizontal plane and $\vec{k}$ was set at 54.7°. The pedestal, supporting the polarimeter, is free to rotate about its own axis, the vertical axis. Data were taken with the polarimeter at the north, east, west, and south positions successively. The Ge(Li) detector and its Dewar are supported by a carriage that rolls on a circular track whose axis of symmetry coincides with the vertical axis. It was always set at 180° from the polarimeter. The axis of each pair of superconducting coils lies in the horizontal plane of the source and intersects at the center of the source and coincides with the north-south and east-west directions.

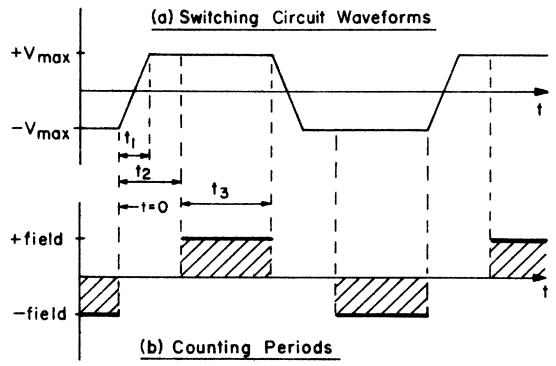


FIG. 4. Switching circuit wave form and counting periods.

A master timer controls the running cycle. With reference to Fig. 4, at $t=0$, it stops the counters and starts the magnet switching circuit, as well as a dead time. The latter is set for a time interval $t_2$ at the end of which the count gates are opened for the next counting period. The output from the switching circuit, and hence the current in the magnet is also shown in Fig. 4. The ramp time $t_1$ is adjustable from 15 sec to 60 sec, but a value of 25 sec was used throughout. Two counting times $t_3$ of 4 min and 10 min were used. The waiting time $t_2$ for the 4 min run was 2 min while that for the 10 min run was 4 min. The choice was based on the spin-lattice relaxation time of $^{57}$Co in iron, which was found to be not more than 30 sec at 18 mK by crude measurements using a multichannel scaler. A waiting time of 4 times the spin-lattice relaxation time was judged to be adequate.

Data were taken for approximately 3 days in each position of the polarimeter. The runs were stopped every 12 hours to fill the liquid nitrogen jacket. The helium reservoir and 1 K pot were replenished every 24 hours. The temperature was measured normally at this time by the method described in Sec. III D. After the 12 days of cold runs in the four positions, the refrigerator was warmed up to 1 K and the "warm" control runs were taken for the same period of time in each position.

### F. Data analysis

For each 12 h period, a series of counts from each of the four single channel analyzers, each set on the scattered peak (Fig. 3) was recorded on paper tape. Let us call the series of numbers $N_1, N_2, \ldots, N_r$, where $N_{2i-1}$ is the number of counts in positive field direction ($\theta = \theta_{max}$) and $N_{2i}$ is the number of counts in negative field direction ($\theta = \pi - \theta_{max}$). The series were corrected for decay (half-life = 270 day). For any three consecutive runs $N_i$, $N_{i+1}$, and $N_{i+2}$, the asymmetry

$$A_i = (-1)^{i+1} \frac{\frac{1}{2}(N_{i+2} + N_i) - N_{i+1}}{\frac{1}{2}(N_{i+2} + N_i) + N_{i+1}} \tag{20}$$

was computed together with its statistical error $\Delta A_i$. The series of $(A_i, \Delta A_i)$ were combined to give the weighted average $\bar{A}$, the statistical error $\Delta \bar{A}$, and the normalized $\chi^2$, taking into account that some data points have been used more than once. This procedure automatically eliminates the linear drifts in count rate. Throughout the experiment, the count rates were very stable so that no higher order trend removal techniques[33] were required (see also Sec. III G). The normalized $\chi^2$ was approximately equal to 1 in all the

runs and hence the statistical error $\Delta\bar{A}$ was equal to that computed from the standard deviation of the distribution. In fact, the normalized $\chi^2$ served as a very sensitive monitor to the experimental conditions during the preliminary trial runs. Whenever the value differed significantly from 1, something had happened during the run such as large temperature fluctutations, equipment failures, etc.

The $\bar{A}$'s of the four NaI detectors were further combined, adjusting for the signs of the asymmetries for detectors Nos. 2 and 4. This is due to the fact that detectors Nos. 1, 2, 3, and 4 were set at $\phi = 45°$, 135°, 225°, and 315°, respectively, and so detectors 2 and 4 were looking at opposite polarization patterns relative to detectors 1 and 3.

### G. Refinements of experimental precision

We see from Eq. (14) that $\Delta(\sin\eta)$ varies as $[-B_3(T)E_p\sqrt{N}]^{-1}$, where $N$ is the count rate. With the aid of the Monte Carlo calculation and several experimental evaluations a conical aluminum scattering block, shown in Fig. 2, was developed that optimized $E_p$.

To obtain the maximum precision, a strong source is needed to increase $N$ subject to two limitations: (a) The concentration of $^{57}$Co in iron must remain sufficiently dilute so as to assure the proper hyperfine fields; (b) the source heating due to $^{57}$Co decay must be within the cooling capacity of the dilution refrigerator.

A careful analysis of the $^3$He and $^4$He mixing characteristics indicated that the refrigerator was working as efficiently as possible. A reevaluation of the thermal shielding of the source rod was made. Several source rod designs were tried in an effort to improve thermal conductivity without increasing the eddy current heating near the superconducting coil pairs.

The tip of the source rod was examined under a microscope, illuminated by a variable strobe light. The tip was vibrating in the horizontal plane with an amplitude of 20 $\mu$m and a frequency of 20 to 30 Hz. Using an accelerometer a study of the entire system, including pumps and cryostat, was made. Vibration sources were reduced by further decoupling them from the refrigerator. The refrigerator still was clamped to the 1 K shield by nylon screws. The upper end of the source rod was buttressed to the mixing chamber centering ring[34] with three brass and Delrin struts. These efforts reduced the vibrations of the tip of the source rod to essentially null.

Initially, using a 2 mCi source, we were able to reach 23 mK, corresponding to a $B_3$ of 0.185. After the optimization program, using the same source, we were able to maintain 17.5 mK with $B_3 = 0.330$.

### H. Possible sources of asymmetries due to imperfect magnetization

We have observed a remanent magnetization in the 90° direction resulting from the source disk having been magnetized in this direction for temperature measurement. To investigate this problem in more detail, the iron disk was first magnetized in the 90° direction in the horizontal plane. The magnetizing current in this direction was decreased slowly through zero to study the effect of this residue field on the 0°–180° field switching time reversal runs. The result is shown in Fig. 5. The asymmetries

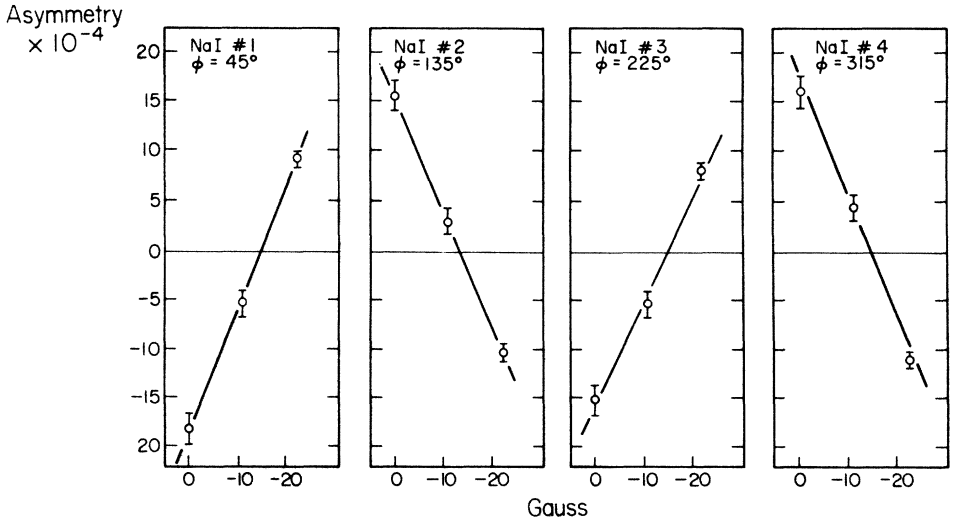


FIG. 5. Asymmetry versus magnetization in the 90° direction in the horizontal plane of the iron disk.

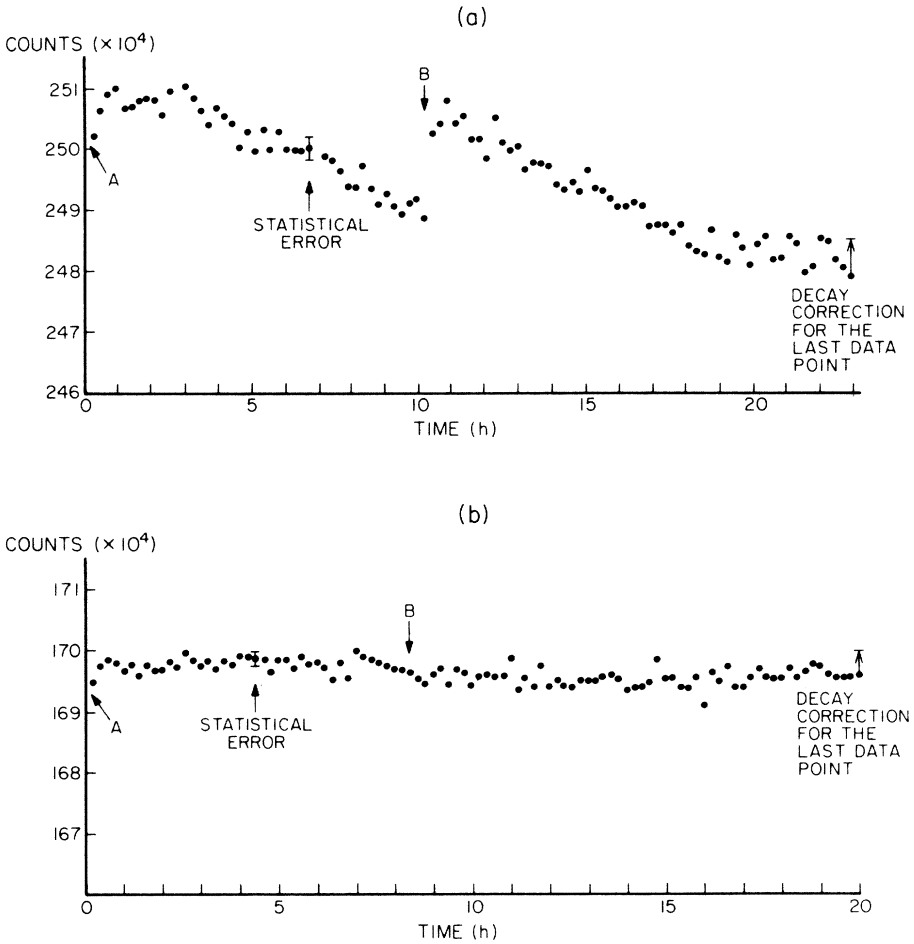


Fig. 6. Plots showing drifts in count rates. (a) Count rate of NaI No. 3 before cryostat was stabilized. Each data point represents a 10 min counting period. (b) Count rates for the same detector after cryostat was stabilized. Each point represents a 4 min counting period, only every other point was plotted [data points have not been corrected for decay in both (a) and (b)].

$$A=\frac{N(\theta=\theta_{max})-N(\theta=\pi-\theta_{max})}{N(\theta=\theta_{max})+N(\theta=\pi-\theta_{max})}$$

varied linearly in the region where the 90° applied field changed sign. The data indicate that the last few strokes of the demagnetization are especially important.

Demagnetization was accomplished by supplying the magnet coils with a sinusoidal current (0.25 Hz) that decreased logarithmically. The demagnetization period was 40 minutes. The first current cycle was 5 A and the last cycle a few $\mu$A.[28]

The effects of a vertical residual magnetic field in the source disk were also investigated. An external coil was wrapped around the room temperature tail piece to induce a vertical field in the source. A small vertical magnetization caused a small asymmetry of the same sign in all four detectors. This asymmetry will not show up in the final result because when we take the average $\bar{A}$ of the four detectors in the way described in Sec. III F, the asymmetries cancel out.[28] Nevertheless, we still wanted to minimize any asymmetry in each NaI detector. The foil was demagnetized manually in the up-down direction with the external coil before a series of runs was started.

### I. Drifts in count rates due to cryogenic liquid levels

With improved precision, after the optimization programs, a variation in the count rates of the NaI detectors with a 12 h periodicity was observed. This is shown in Fig. 6(a). At point A a helium and nitrogen transfer was made at midnight and at point B a nitrogen transfer was made the following noon. For comparison, the decay correction and the statistical error are also indicated. The change in count rate when helium was transferred

TABLE I. Summary of experimental results. Polarization efficiency $E_p = -0.456 \pm 0.009$. $\chi^2$ per degree of freedom $= 0.95$. $P(X_\nu^2 > 0.95) = 0.55$. No. of degrees of freedom $= 26$.

| | Mean temperature (mK) | Mean $B_3$ | Raw asymmetry $A'$ ($\times 10^{-5}$) | Corrected asymmetry $A$ ($\times 10^{-5}$)[a] | $\sin\eta$ ($\times 10^{-4}$) |
|---|---|---|---|---|---|
| North position | 17.5 | 0.316 | 0.3±1.7 | 0.3±1.8 | 2.4±15.1 |
| South position | 17.7 | 0.312 | 0.0±1.3 | 0.0±1.4 | 0.2±11.7 |
| East position | 17.9 | 0.304 | 0.4±1.5 | 0.4±1.5 | 3.4±13.3 |
| West position | 17.2 | 0.325 | −2.0±1.5 | −2.1±1.6 | −17.0±12.8 |
| Weighted average of the four positions | 17.6 | 0.313 | −0.35 ± 0.74 | −0.37 ± 0.78 | −3.1±6.5 |

[a]Corrected asymmetry $A$ is related to raw asymmetry $A'$ by $A = A'(1+f)$ with $1+f = 1.06 \pm 0.02$.

was due to a slight warmup of the refrigerator and that when nitrogen was transferred was due to a sudden change in weight of the liquid nitrogen jacket. As liquid nitrogen was boiling off, the cryostat moved through a small angle relative to the polarimeter, causing a tiny change in solid angle of the detector system. To overcome this problem the cryostat was fastened to the circular track, which supports the polarimeter, by three aluminum struts and the drift was essentially removed [Fig. 6(b)].

## IV. RESULTS

After the various problems described in Sec. III were overcome, the final series of runs were made. Data were taken in all four positions (north,

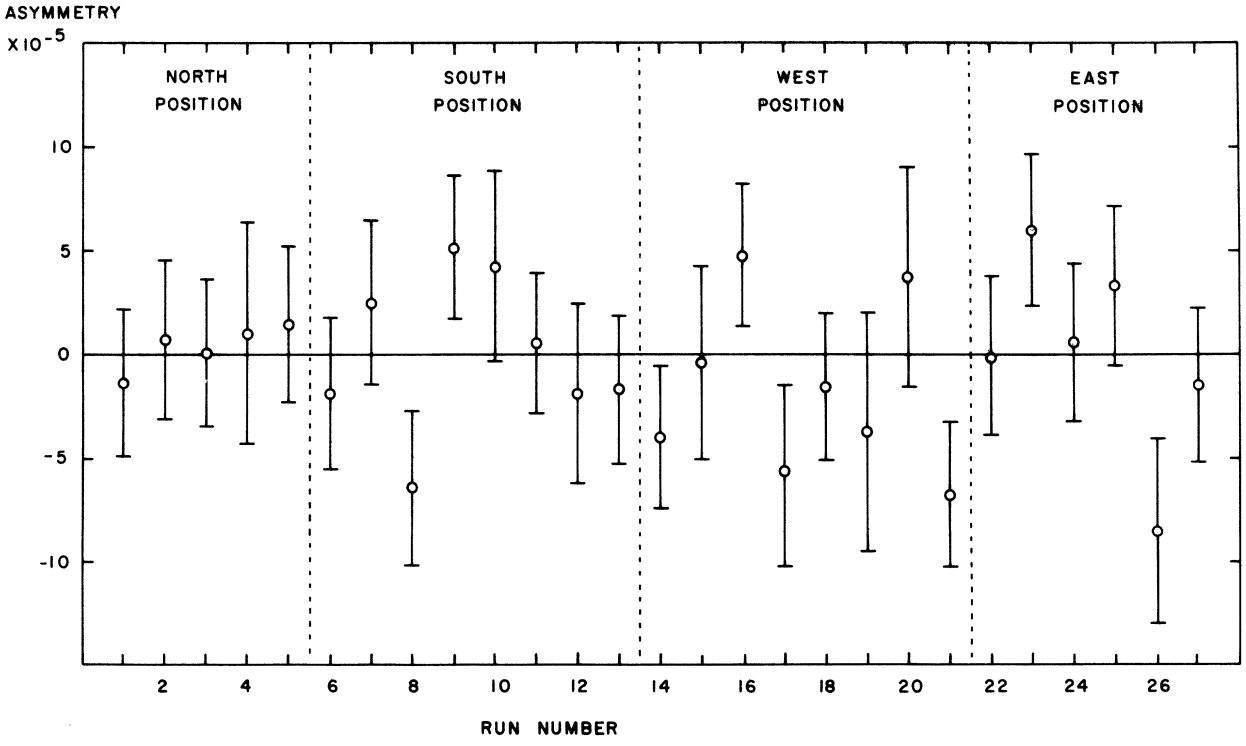


FIG. 7. Asymmetries of 27 runs, each of roughly 12 h duration.

TABLE II. Results of 1 K control runs.

| | Asymmetry ($\times 10^{-5}$) |
|---|---|
| North position | 0.6±2.0 |
| South position | 1.0±1.9 |
| East position | 5.6±2.9 |
| West position | −0.9±1.9 |
| Weighted average of 4 positions | 0.93 ± 1.04 |

west, south, and east) around the vertical axis of the refrigerator for roughly equal periods of time. Results for 14 days of data taken are summarized in Table I and the asymmetries for the 27 consecutive runs, each of approximately 12 h duration, are plotted in Fig. 7. No rejection of data was made.

An equal number of 1 K runs were made at identical geometry after the 14 days of cold runs. The results are given in Table II. No net asymmetry was observed. Numerous 1 K runs have been made in all four positions at various stages of the experiment before the final series of data runs. The results are all consistent with a null asymmetry. For these reasons, we conclude that there was no systematic asymmetry at 1 K and no subtraction of warm runs from cold runs was made.

The final value $\sin\eta = (-3.1 \pm 6.5) \times 10^{-4}$ will be adopted for subsequent discussions.

## V. NUCLEAR AND ATOMIC EFFECTS THAT SIMULATE *T* VIOLATION

In measurements involving small asymmetries of ~$10^{-5}$, apart from the various systematic instrumental errors as described in the previous sections, it is hardly surprising that some small nuclear and atomic effects might show up which will mask the genuine effects we are seeking. We shall discuss two possibilities in this section.

### A. Faraday effect from ferromagnets

The linearly polarized $\gamma$ rays from $^{57}$Co decay pass through a certain thickness of the ferromagnetic iron before reaching the polarimeter. The polarization dependence of the refractive index $n$ of a magnetized optical medium causes a rotation of the polarization vector $\vec{E}$. This would be recorded in the polarimeter as an asymmetry. Bock and Luksh[35,36] have studied this problem and they measured the angle of rotation for iron to be $\Omega_0 = (3.9 \pm 0.3) \times 10^{-3}$ rad cm$^{-1}$, which agreed quite well with theory.

Using this value of $\Omega_0$, we see that in our experiment, the expected asymmetry would be given by

$$A \simeq B_2 U_2 A_{22} P_2^2(\cos 54.7^\circ)(2\Omega) E_p , \tag{21}$$

where $\Omega \simeq \Omega_0 t \cot 54.7^\circ$, $t$ being the thickness of the foil. At 17.5 mK, this corresponds to $A \sim 6 \times 10^{-7}$, which is more than an order of magnitude below the resolution of the present experiment. Hence this effect can be safely neglected. (This effect is important for scattering type experiments such as in a Mössbauer experiment, where the polarized $\gamma$ rays have to pass through a thicker ferromagnet.)

### B. Final state interactions

Henley and Jacobsohn[37] have studied the magnitude of the terms in angular distributions which would mimic $T$-violation effects. They pointed out that in calculating angular distributions, the electromagnetic matrix elements are evaluated in Born approximation and are, therefore, Hermitian. If higher order terms are considered, the transition operator is no longer Hermitian and apparent $T$-violation terms can occur. In general, the transition operator $S$ has both a Hermitian and an anti-Hermitian component:

$$S = \tfrac{1}{2}(S + S^\dagger) + \tfrac{1}{2}(S - S^\dagger) = S^h + S^a . \tag{22}$$

Even if there are no $T$-violating terms, higher order contributions to $S$ can lead to a nonvanishing component $S^a$ and simulate $T$ violation. The contributing Feynman diagrams are shown in Figs. 8(b) to 8(g) in addition to the basic photon emission process of Fig. 8(a). Taking these diagrams into account, the reduced matrix element $\langle f \| A(L,\pi) \| i \rangle$ has to be replaced by

$$\langle f \| A'(L,\pi) \| i \rangle = (1 + E_L^\pi) \langle f \| A(L,\pi) \| i \rangle , \tag{23}$$

where $E_L^\pi$ is a complex quantity whose magnitude is much less than 1. Putting $\xi_L^\pi = \mathrm{Im} E_L^\pi$ we then have

$$\langle f \| A'(L,\pi) \| i \rangle \simeq (1 + i\xi_L^\pi) \langle f \| A(L,\pi) \| i \rangle$$

$$\simeq e^{i\xi_L^\pi} \langle f \| A(L,\pi) \| i \rangle , \tag{24}$$

and the modified mixing ratio $\delta'$ is

$$\delta' = \delta e^{i\xi} = |\delta'| e^{i(\xi+\eta)} , \tag{25}$$

where $\xi = \xi_L^\pi - \xi_L^{\pi\prime}$, $\eta = \eta_L^\pi - \eta_L^{\pi\prime}$. Hence our measured quantity will be $\sin(\xi + \eta)$ rather than $\sin\eta$.

Henley and Jacobsohn[37] estimated that the nuclear

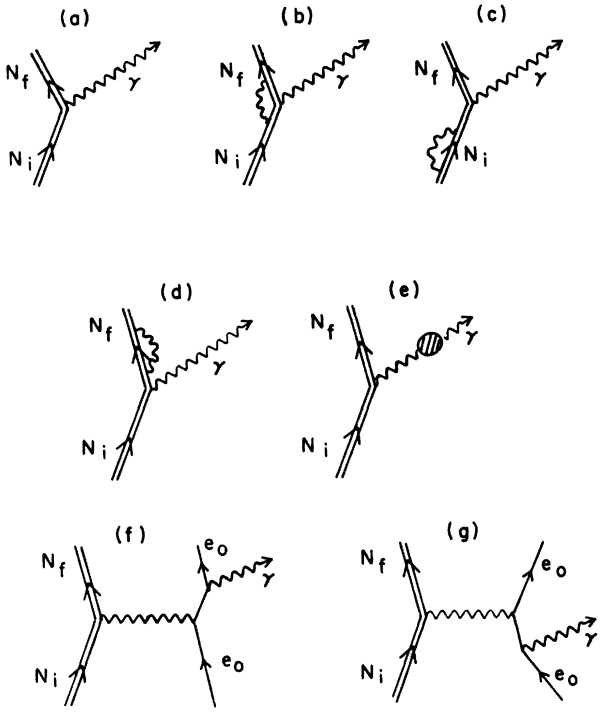


FIG. 8. Diagrams contributing to the process $N_i \rightarrow N_f + \gamma$ to order $e\alpha$. The single lines represent the electrons and the double lines the nucleus state. The blob in diagram (e) represents the lowest order (in the electromagnetic coupling) corrections to the photon propagator.

radiative correction [Figs. 8(b) to (e)] give a contribution to $\xi$ of the order of magnitude $10^{-6}$ to $10^{-7}$. This contribution is relatively small (compared with the fine structure constant $\alpha$) because the matrix elements corresponding to intermediate states involving real photons contain retardation factors of the order $(kR)^L$, where $k$ is the wave number of the photon and $L$ the multipolarity. $R$ is the dimension of the radiative source and is much smaller for a nucleus than for an atom. This effect is hence beyond the sensitivity of the present experiment and can be safely ignored.

Hannon and Trammel[38,39] and Goldwire and Hannon[40] have studied the higher order effects corresponding to processes involving the atomic electrons [Figs. 8(f) and 8(g)]. The absorptive parts of these diagrams correspond to the $|e'N_f\rangle$ and $|e_0 N_f \gamma\rangle$ intermediate states in the unitarity relation.[41] $|N_f\rangle$ is the final nuclear state, $|e_0\rangle$ represents an initial bound electron state, and $|e'\rangle$ represents a continuum energy electron state. The following approximate relations can be derived for the contribution of these states to the phases $\xi_L^\pi$ (see Refs. 42, 43)

$$\begin{aligned} \xi_L^\pi(e'N_f) &= \epsilon[\alpha_{\text{int}}\sigma_p(L,\pi)/(4L+2)\pi\lambda_0{}^2]^{1/2}, \\ \xi_L^\pi(e_0 N_f\gamma) &= \tilde{\epsilon}[\sigma_e(L,\pi)/(4L+2)\pi\lambda_0{}^2]^{1/2}, \end{aligned} \tag{26}$$

where $\alpha_{\text{int}}$ is the internal conversion coefficient, $\sigma_p(L,\pi)$ is the partial cross-section for $(L,\pi)$ photoelectric emission, $\sigma_e(L,\pi)$ is the partial cross-section for the $EL$ or $ML$ contribution to elastic photon-electron scattering (Thomson effect), $\lambda_0$ is the wavelength of the emitted $\gamma$ ray, and $\epsilon$ and $\tilde{\epsilon}$ are real numbers with absolute values slightly less than one.

Goldwire and Hannon[40] have made detailed calculations of the phases $\xi_L^\pi(e'N_f)$ and $\xi_L^\pi(e_0 N_f\gamma)$. Applying their results for the 122 keV $M1$-$E2$ transition, we get

$$\xi_1^M(K, L \text{ conversion}) = -0.27\times10^{-4},$$

$$\xi_2^E(K, L \text{ conversion}) = -7.92\times10^{-4},$$

$$\xi_1^M(\text{Thomson}) = -7.3\times10^{-4},$$

$$\xi_2^E(\text{Thomson}) = -5.6\times10^{-4},$$

$$\begin{aligned} \xi &= [\xi_2^E(\text{conversion}) - \xi_1^M(\text{conversion})] \\ &\quad + [\xi_2^E(\text{Thomson}) - \xi_1^M(\text{Thomson})] \\ &= (-6.0\pm0.4)\times10^{-4}, \end{aligned}$$

where the error is the estimated cumulative computational error. The value of $\xi$ is of the order of the precision in the present experiment. If one accepts the above value of $\xi$, the measured value then becomes

$$\sin(\eta+\xi) = (-3.1\pm6.5)\times10^{-4}$$

or

$$\sin\eta = (2.9\pm6.6)\times10^{-4}.$$

## VI. DISCUSSION AND CONCLUSION

The present experimental result, $\sin(\eta+\xi) = (-3.1 \pm 6.5)\times10^{-4}$, is consistent with time reversal invariance to 7 parts in $10^4$. In view of this result, the classes of millistrong and electromagnetic theories of $CP$ violation which predict manifestations of $10^{-3}$ have a somewhat weaker stand, although they are by no means ruled out. It is, of course, assumed that the $CPT$ theorem is valid. The next class of theories would be the milliweak theories, their manifestations would be at least one and a half orders of magnitude below the present experimental precision.

A comparison of the present value with other measurements in $\gamma$-decay is given in Table III. All these values are consistent with the most recent limit on the neutron dipole moment[44] as far as its implication on time reversal invariance is concerned. We must note that the observables measured in the neutron dipole moment case are

TABLE III. Summary of experimental data.

| Nucleus | Method [a] | Cascade (keV) | $\delta$ [b] | $10^3 \times \sin\eta$ | Reference |
|---|---|---|---|---|---|
| $^{36}$Cl | $n$-$\gamma$-$\gamma$ | 7790-790 | 0.21 | $4 \pm 12$ | Eichler (12) |
| $^{36}$Cl | $n$-$\gamma$-$\gamma$ | 7790-790 | 0.21 | $-1.8 \pm 2.2$ | Bulgakov *et al.* (13) |
| $^{49}$Ti | $n$-$\gamma$-$\gamma$ | 341-1378 | 0.1 | $17 \pm 25$ | Kajfosz *et al.* (14) |
| $^{56}$Fe | $\beta$-$\gamma$-$\gamma$ | 2110-847 | 0.18 | $4 \pm 26$ | Garrell *et al.* (9) |
| $^{56}$Fe | $\beta$-$\gamma$-$\gamma$ | 1811-847 | -0.28 | | |
| $^{57}$Fe | $J$-$\gamma$-$\epsilon$ | 122 | 0.12 | $-0.31 \pm 0.65$ | Present work |
| $^{99}$Ru | M.E. | 90 | -1.65 | $1.0 \pm 1.7$ | Kistner (18) |
| $^{106}$Pd | $\beta$-$\gamma$-$\gamma$ | 1050-512 | 0.21 | $30 \pm 40$ | Fuschini *et al.* (10) |
| $^{106}$Pd | $\beta$-$\gamma$-$\gamma$ | 1050-512 | 0.21 | $4 \pm 18$ | Perkins and Ritter (11) |
| $^{169}$Tm | $J$-$\gamma$-$\gamma$ | 198-110 | -0.30 | $150 \pm 120$ | Murdoch *et al.* (17) |
| $^{169}$Tm | $J$-$\gamma$-$\gamma$ | 177-130 | -0.51 | $\geq 0$ | Murdoch *et al.* (17) |
| $^{175}$Lu | $J$-$\gamma$-$\gamma$ | 283-114 | -0.036 | $170 \pm 500$ | Murdoch *et al.* (17) |
| $^{180}$Hf | $J$-$\gamma$-$\gamma$ | 501-332 & 215 | 5.3 | $48 \pm 87$ | Krane *et al.* (16) |
| $^{193}$Ir | M.E. | 73 | 0.56 | $0.2 \pm 3.8$ | Atac *et al.* (19) |
| $^{193}$Ir | M.E. | 73 | 0.56 | $0.7 \pm 2.4$ | Zech *et al.* (20) |
| $^{192}$Pt | $J$-$\gamma$-$\gamma$ | 604-316 | -2.1 | $4 \pm 5$ | Holmes *et al.* (15) |

[a] M.E. stands for Mössbauer effect.
[b] All mixing is $E2$-$M1$ except in $^{175}$Lu($E1$-$M2$) and $^{180}$Hf($E3$-$M2$).

$P$-odd and $T$-odd, whereas in the $\gamma$-decay case $P$-even $T$-odd observables are measured. Thus in order to allow a comparison between theory and experiment one needs a more precise estimate within a particular theoretical framework on the size of the expected theoretical effects with a specific symmetry (i.e., whether one is comparing $P$-even $T$-odd terms or $P$-odd $T$-odd terms).

In conclusion, by measuring the linear polarization of the 122 keV $\gamma$ rays from $^{57}$Co oriented in iron, we have determined a value of $\sin\eta = -(3.1 \pm 6.5) \times 10^{-4}$. This result is consistent with and about half an order of magnitude more precise than all previous experimental values in low energy nuclear physics, and is consistent with time reversal being invariant. The theoretical significance of the present experimental result should be pursued.

This experiment marked a significant improvement in statistical accuracy over the previous work because it is essentially a single counting experiment compared to the older coincidence experiments. However, one is left to measure the relatively insensitive $k=3$ term instead of the more sensitive $k=1$ term in the angular distributions. In addition, the poor energy resolution inherent in the linear polarimeter limits this technique to cases where the $\gamma$ ray spectrum is simple.

Through the present experiment, an immense amount of experience has been gained in the technique for measuring the linear polarization of $\gamma$ rays from oriented nuclei to high precision. This technique will be utilized to pursue other cases of interest.

## ACKNOWLEDGMENTS

We would like to thank Dr. A. J. Becker, Dr. E. J. Cohen, Dr. D. Cook, and Dr. E. Seltzer for their contributions in the early part of the project. We are very much indebted to Dr. H. C. Goldwire and Dr. J. P. Hannon for communicating their results to us prior to publication, and Dr. P. Herczeg for very helpful discussions. The assistance of Mr. E. Redden and Mr. J. L. Gimlett with the apparatus is gratefully acknowledged.

*Present address: Bell Laboratories, Holmdel, New Jersey 07733.
†Work supported by ERDA EY-76-C-03-0063.
[1] J. H. Christenson, J. W. Conin, V. L. Fitch, and R. Turlay, Phys. Rev. Lett. 13, 138 (1964).
[2] R. C. Casella, Phys. Rev. Lett. 21, 1128 (1968); 22, 554 (1969).
[3] A review of the present situation is given by K. Kleinknecht, Annu. Rev. Nucl. Sci. 26, 1 (1976).
[4] S. P. Lloyd, Phys. Rev. 81, 161 (1951).
[5] E. M. Henley, Annu. Rev. Nucl. Sci. 19, 367 (1969).
[6] R. J. Blin-Stoyle, *Fundamental Interactions and the Nucleus* (North-Holland, Amsterdam, 1973).
[7] B. A. Jacobsohn and E. M. Henley, Phys. Rev. 113, 234 (1959).
[8] F. Boehm, in *Hyperfine Structure and Nuclear Radiations*, edited by E. Matthias and D. A. Shirley (North-Holland, Amsterdam, 1968), p. 279.
[9] M. Garrell, H. Frauenfelder, D. Ganek, and D. C. Sutton, Phys. Rev. 187, 1410 (1969).

[10]E. Fuschini, V. Gadjokov, C. Maroni, and P. Veronesi, Nuovo Cimento 33, 709, 1309 (1964).
[11]R. B. Perkins and E. T. Ritter, Phys. Rev. 174, 1426 (1968).
[12]J. Eichler, Nucl. Phys. A120, 535 (1968).
[13]M. I. Bulgakov, A. D. Gulko, G. V. Danilyan, I. L. Karphikin, P. A. Krupchitskii, V. V. Novitskii, Yu. A. Oratovskii, V. S. Pavlov, E. I. Tarkovskii, and S. S. Trostin, Yad. Fiz. 18, 12 (1973) [Sov. J. Nucl. Phys. 18, 6 (1974)].
[14]J. Kajfosz, J. Kopecký, and J. Honzáko, Nucl. Phys. A120, 225 (1968).
[15]M. J. Holmes, W. D. Hamilton, and R. A. Fox, Nucl. Phys. A199, 401 (1973).
[16]K. S. Krane, B. T. Murdoch, and W. A. Steyert, Phys. Rev. C 10, 840 (1974).
[17]B. T. Murdoch, C. E. Olsen, and W. A. Steyert, Phys. Rev. C 10, 1475 (1974).
[18]O. C. Kistner, Phys. Rev. Lett. 19, 872 (1967); in *Hyperfine Structure and Nuclear Radiations* (see Ref. 8), p. 295.
[19]M. Atac, B. Chrisman, P. Debrunner, and H. Frauenfelder, Phys. Rev. Lett. 20, 691 (1968).
[20]E. Zech, F. Wagner, H. J. Koerner, and P. Kienle in *Hyperfine Structure and Nuclear Radiations* (see Ref. 8), p. 314; E. Zech, Z. Phys. 239, 197 (1970).
[21]N. K. Cheung, H. E. Henrikson, E. J. Cohen, A. J. Becker, and F. Boehm, Phys. Rev. Lett. 37, 588 (1976).
[22]R. M. Steffen, Los Alamos Scientific Laboratory Report No. LA-4565-MS, 1971 (unpublished).
[23]R. M. Steffen and K. Alder, in *The Electromagnetic Interactions in Nuclear Spectroscopy*, edited by W. D. Hamilton (North-Holland, Amsterdam, 1975), p. 505.
[24]K. S. Krane, Los Alamos Scientific Laboratory Report No. LA-4677, 1971 (unpublished).
[25]K. S. Krane, Nucl. Data Tables 11, 407 (1973).
[26]E. J. Cohen, A. J. Becker, N. K. Cheung, and H. E. Henrikson, Hyperfine Interactions 1, 193 (1975).
[27]G. N. Rao, in Report on International Meeting on Hyperfine Interactions, University of Leuven, Belgium, 1975 (unpublished).
[28]N. K. Cheung, Ph.D. thesis, 1976, California Institute of Technology (unpublished).
[29]ICN Isotope and Nuclear Division, 2727 Campus Drive, Irvine, California 92664.
[30]A. J. Becker, H. E. Henrikson, and D. C. Cook, Nucl. Instrum. 108, 291 (1973).
[31]B. A. Logan, R. T. Jones, and A. Ljubičić, Nucl. Instrum. 108, 603 (1973).
[32]C. M. Lederer, J. M. Hollander, and I. Perlman, *Table of Isotopes* (Wiley, New York, 1967).
[33]D. W. Cruse and W. D. Hamilton, Nucl. Instrum. 57, 29 (1967).
[34]H. E. Henrikson, Rev. Sci. Instrum. 42, 1533 (1971).
[35]P. Bock and P. Luksh, Nuovo Cimento Lett. 2, 1081 (1971).
[36]P. Bock and P. Luksh, Z. Phys. 263, 147 (1973).
[37]E. M. Henley and B. A. Jacobsohn, Phys. Rev. Lett. 16, 706 (1966).
[38]J. P. Hannon and G. T. Trammel, Phys. Rev. Lett. 21, 726 (1968).
[39]J. P. Hannon and G. T. Trammel, Phys. Rev. 186, 306 (1969).
[40]H. C. Goldwire and J. P. Hannon, Phys. Rev. (to be published).
[41]We follow here the exposition in a review by F. Boehm, P. Herczeg, W. A. Steyert, and W. Weyhmann, Phys. Rep. (to be published).
[42]G. T. Trammel and J. P. Hannon, Phys. Rev. 180, 337 (1969).
[43]Yu. M. Kagan, A. M. Afanas'ev, and V. K. Voitovetskii, Zh. Eksp. Teor. Fiz. Pis'ma Red. 9, 155 (1969) [JETP Lett. 9, 91 (1969)].
[44]N. F. Ramsey, Bull Am. Phys. Soc. 21, 61 (1976), Ser. II.